Spanish Journal of Agricultural Research
16 (4), e0204, 15 pages (2018)
eISSN: 2171-9292
https://doi.org/10.5424/sjar/2018164-11185
Instituto Nacional de Investigación y Tecnología Agraria y Alimentaria, O.A, M.P. (INIA)

RESEARCH ARTICLE

OPEN ACCESS

An automatic and non-intrusive hybrid computer vision system for the estimation of peel thickness in Thomson orange

Hossein Javadikia[1], Sajad Sabzi[2] and Juan I. Arribas[3,4]

[1]Razi University, College of Agriculture and Natural Resources, Dept. Mechanical Engineering of Biosystems, Kermanshah, Iran. [2]University of Mohaghegh Ardabili, College of Agriculture, Dept. Biosystems Engineering, Ardabil, Iran. [3]University of Valladolid, Dept. Teoría de la Señal y Comunicaciones, 47011 Valladolid, Spain. [4]University of Salamanca, Instituto de Neurociencias de Castilla-León, 37007 Salamanca, Spain.

Abstract

Orange peel has important flavor and nutrition properties and is often used for making jam and oil in the food industry. For previous reasons, oranges with high peel thickness are valuable. In order to properly estimate peel thickness in Thomson orange fruit, based on a number of relevant image features (area, eccentricity, perimeter, length/area, blue component, green component, red component, width, contrast, texture, width/area, width/length, roughness, and length) a novel automatic and non-intrusive approach based on computer vision with a hybrid particle swarm optimization (PSO), genetic algorithm (GA) and artificial neural network (ANN) system is proposed. Three features (width/area, width/length and length/area ratios) were selected as inputs to the system. A total of 100 oranges were used, performing cross validation with 100 repeated experiments with uniform random samples test sets. Taguchi's robust optimization technique was applied to determine the optimal set of parameters. Prediction results for orange peel thickness (mm) based on the levels that were achieved by Taguchi's method were evaluated in several ways, including orange peel thickness true-estimated boxplots for the 100 orange database and various error parameters: the sum square error (SSE), the mean absolute error (MAE), the coefficient of determination (R^2), the root mean square error (RMSE), and the mean square error (MSE), resulting in mean error parameter values of R^2=0.854±0.052, MSE=0.038±0.010, and MAE=0.159±0.023, over the test set, which to our best knowledge are remarkable numbers for an automatic and non-intrusive approach with potential application to real-time orange peel thickness estimation in the food industry.

Additional keywords: machine learning; neural network; particle swarm optimization; stochastic analysis; peel thickness, skin.

Abbreviations used: ANN (Artificial Neural Networks); GA (Genetic Algorithm); GMDH (Group Methods od Data Handling-type); IPSO (Improved Particle Swarm Optimization); LSSVR (Least Squartes Support Vector Regression); PSO (Particle Swarm Optimization); SNR (Signal to Noise Ratio); SVM (Support Vector Machine); TA (Titratable Acidity); TSS (Total Soluble Solids).

Authors' contributions: All authors conceived, designed and performed the experiments, analysed the data, participated in the revision of scientific content, the drafting of the paper, and read and approved the final manuscript.

Citation: Javadikia, H.; Sabzi, S.; Arribas, J. I. (2018). An automatic and non-intrusive hybrid computer vision system for the estimation of peel thickness in Thomson orange. Spanish Journal of Agricultural Research, Volume 16, Issue 4, e0204. https://doi.org/10.5424/sjar/2018164-11185

Supplementary material (Fig. S1) accompanies the paper on SJAR's website.

Received: 10 Feb 2017. **Accepted:** 12 Nov 2018.

Funding: Vice Chancellor for Research and Technology of Razi University, Iran (PP49_6).

Competing interests: The authors have declared that no competing interests exist.

Correspondence should be addressed to Juan-Ignacio Arribas: jarribas@tel.uva.es, or Hossein Javadikia: pjavadikia@gmail.com (shared corresponding authors).

Introduction

Thomson orange (*Citrus sinensis* (L.) Osbeck) is a delicious fruit consumed worldwide. While originated in Southeast Asia, it is widely grown in Brazil, USA, India, Mexico, China, Spain, Italy, Iran, Egypt, and Pakistan, among others. It is consumed directly as fresh and fresh juice or indirectly as jam or oil. According to the statistics published, Iran is known as the sixth citrus producer around the world (Adelkhani *et al.*, 2013). Orange peel has valuable flavor and nutrition properties, and is often used to make jam and oil. Orange peel can be either thick or thin. For obvious reasons, oranges with more peel thickness have more oil and can produce more jam. Grading peel of fruits provides information with regard to its thickness. The use of machine vision techniques for processing of vegetables and fruits has increased during last two decades. Nowadays, many producers around the world build grading machines capable of pre-grading fruits by mass, color, size and

skin (Blasco *et al.*, 2003). For example, Fu *et al.* (2016) graded kiwifruit based on shape features using a single camera. For this aim an image processing algorithm was designed. Several features were used, including length, maximum diameter of the equatorial section, and projected area were extracted from kiwi fruits. Results showed that based on length and weight, volume value can be predicted, since real and predicted volumes had a good agreement with a coefficient of determination of 0.98. Thendral & Suhasini (2017) analyzed orange skin for grading purposes based on skin defect using machine vision including color and texture features. Three classifiers, back propagation neural network, support vector machine and auto associative neural network (AANN), were used. Results showed that AANN had best results among these three classifiers with an accuracy of 94.5%. Naganur *et al.* (2012) proposed a method based on fuzzy logic and image processing to grade six types of fruits, including orange, apple, sweet lime, banana, banana (Rasaballe) and guava. Grading was performed based on area and major axis, resulting in a good accuracy classification. Determining a proper relationship between orange peel thickness and morphological characteristics may therefore be useful and applicable in non-intrusive peel thickness grading.

Next, a state of the art in automatic orange, citrus or other fruits computer vision systems and peel thickness estimation is presented, which to our best knowledge is rather novel as of today. Fan *et al.* (2013) studied on surface images with texture characteristics of 17 samples and 25 different parts were detected within one sample using a computer vision system, including texture profile analysis in extruded food (rice). According to the linear fitting model, the hardness and gumminess score can be reflected directly by the a^* and intensity based on correlation coefficient of 0.9558, 0.9741 and 0.9429, 0.9619, respectively. Leiva-Valenzuela *et al.* (2013) predicted firmness and soluble solids content of blueberries using hyperspectral reflectance imaging. A pushbroom hyperspectral imaging system was used to acquire hyperspectral reflectance images from 302 blueberries in two fruit orientations (*i.e.*, stem and calyx ends) for the spectral region of 500–1000 nm. Liu *et al.* (2013) studied on prediction of dissolved oxygen content in river crab culture based on least squares support vector regression optimized by improved particle swarm optimization (PSO). In this work, authors present a hybrid dissolved oxygen content prediction model based on the least squares support vector regression (LSSVR) model with optimal parameters selected by improved particle swarm optimization (IPSO) algorithm. In view of the slow convergence of PSO, IPSO was proposed with the dynamically adjusted inertia weight based on the fitness function value in order to improve convergence. Then a global optimizer IPSO was employed to optimize the hyper-parameters needed in the LSSVR model. Shin *et al.* (2012) investigated postharvest citrus mass and size estimation using a logistic classification model and a watershed algorithm. An image processing algorithm was developed to identify fruit from images of the postharvest citrus from a commercial citrus grove. For fruit detection, logistic regression model based pixel classification algorithms were developed. To avoid misclassification due to highly saturated area on fruit and non-fruit regions, a highly saturated area recovering algorithm was developed that avoided the use of a "filling holes" operation. Tong *et al.* (2013) conducted a study on developing machine vision techniques for the evaluation of seedling quality based on leaf area. Leaf area of a seedling is an important indicator of its quality. Here, a vision system was used to measure the leaf area in each cell to distinguish "bad" and "good" plugs. Based on the principle of proportion in area, the procedures for processing top-view seedling images and a method for calculating the leaf area of each seedling in the plug tray were investigated. Marchal *et al.* (2013) investigated an expert system based on computer vision to estimate the content of impurities in olive oil samples. In particular, authors developed a system based on computer vision and pattern recognition to classify the content of impurities of the olive oil samples in three sets, indicative of the goodness of the separation process of olive oil after its extraction from the paste. Starting from the histograms of the Red–Green–Blue channels for the RGB, CIELAB and Hue–Saturation–Value (HSV) color spaces, they constructed an initial input parameter vector and performed a feature extraction step previous to the classification phase. Several linear and non-linear feature extraction techniques were evaluated, and the classifiers used were support vector machines (SVMs) and ANN. The best correct classification rate (CCR) they achieved was 87.66%, obtained using kernel Principal Component Analysis and a grade-3-polynomial kernel SVM.

Mottaghitalab *et al.* (2015) predicted the content of two chemical compounds: methionine and lysine related to soybean and fish meal, based on neural networks. For this aim, 119 and 116 data line from methionine and lysine, respectively, were used to develop Group Method of Data Handling-type (GMDH) neural network models. Results show that the GMDH had suitable performance. Karimi *et al.* (2015) proposed a new method based on an acoustic technique to evaluate seeding properties in laboratory. To that end they used three different seeds including corn, wheat and Pelleted tomato. In their proposed method, seeds were detected based on a rising voltage value that a microphone sensed

over each impaction of seeds to a steel plate. Results show that the coefficient of determination between gathered data from a belt system and the corresponding seeds spacing measured with the acoustic system, was 0.98 on average. Rungpichayapichet *et al.* (2017) focused over the prediction of physicochemical features of mango fruits including, firmness, total soluble solids (TSS) and titratable acidity (TA) based on hyperspectral images. Predicted models were developed based on spectral data in visible and infrared ranges, using partial least squares regression. Results showed that there exists a high correlation between hyperspectral images and firmness, TSS and TA, so that the values of the determination coefficient and root mean square error (RMSE) between hyperspectral images and firmness, TSS and TA, were 0.81, 2.83 and 0.5 (determination coefficients), and 2, 0.81 and 0.24 (RMSEs), respectively. Mohapatra *et al.* (2017) provided a method for grading the ripening steps of red banana using the changes in the dielectric properties as well as image processing procedures. Fruits were stored at a temperature of 25 °C during transportation. The test was carried out in a ripening chamber with fruits stored at a relative humidity level of 85-88% different treatment temperatures of 15.5, 22 and 28 °C, control temperature (30 ± 2 °C), for 14, 9, 8 and 7 days, respectively. Dielectric characteristics such as capacitance, relative permittivity and impedance change were measured during the ripening process. In the next step, 140 images (20 images for each ripening step) were prepared vertically using a camera under natural light at a height of 30 cm. Two classifiers were used: (a) Chi-Square distance/nearest neighbor, and (b) Fuzzy C means (FCM) clustering. Results showed that different stages of ripening were classified with high accuracy under the proposed system.

The aim of this study was to identify orange peel thickness using computer vision and artificial intelligence techniques. Artificial intelligence term was introduced by John McCarthy in 1956. He defined it as "the science and engineering of making intelligent machines, especially intelligent computer programs". Artificial intelligence can be divided into four groups: (1) systems that think similar to humans, (2) systems that work similar to humans, (3) systems that think logical, and (4) systems that work logical (Mellit & Kalogirou, 2014).

Traditionally, machine vision techniques are divided into two parts: image processing and data analysis. In turn, there are two subparts inside image processing: hardware and software systems. Hardware systems consist of an image acquisition system, camera, frame grabber and personal computer (PC). On the other hand, software systems include optimal programming to properly extract morphological and color characteristics of an interest object.

The objectives of this work were: (i) to predict Thomson orange peel thickness from visual image features using non-intrusive computer vision techniques, in the visual range; (ii) to get an optimal use of oranges, in a way that each and every orange that has a thick skin, its peel is used for jam and pomace use for fruit juice; otherwise it is used for fresh eating; and (iii) to propose an effective and as simple as possible machine vision system prototype for potential use in a processing factory under real environment conditions.

Material and methods

Material

In this study, 100 Thomson orange samples were randomly selected and transferred to the Department of Mechanical Engineering of Biosystems, Razi University, Kermanshah, Iran. Selecting samples were among those healthy and free from any injuries recollected from orchards in the North of Iran. Eighty percent of oranges (80 oranges) were used as training samples and 20% remaining (20 oranges) as testing samples. In order to obtain statistical valid results, experiments were uniform random repeated 100 times, resulting in 2000 test oranges; each different orange sample number (orange # in what follows) was used 20 times on average over the test set. At the same time, true orange peel thickness was measured by using a digital caliper (Guanglu, China,) with an accuracy of 10 μm.

Illumination, data acquisition and image segmentation

Image data acquisition and illumination conditions

The proposed machine vision system (Fig. 1), consists of a digital camera (BOSCH, Portugal), an image acquisition system, a frame grabber (Pinnacle, China) and a PC, 2.27GHz Intel(R) Core(TM) i3 CPU and 4 GB of RAM memory, which has been equipped with MatLab program (ver. R2014a, MathWorks, Natick, MA, USA). The system provides images with a medium resolution of 352 × 288 pixels, so as to allow easy real time potential industrial application. The image acquisition system includes three types of lamps: fluorescent, LED, and tungsten. The lamps were arranged in three rows along each lateral plane of a cubic chamber. Fluorescent lamps have predominant white light while tungsten bulbs have red, yellow and pink wavelength lights. Each set of LED lamps comprises five rows consisting of 40 LED lamps each. Light temperatures of LED lamps were orange, blue, red, white and green, rows from top to bottom. The

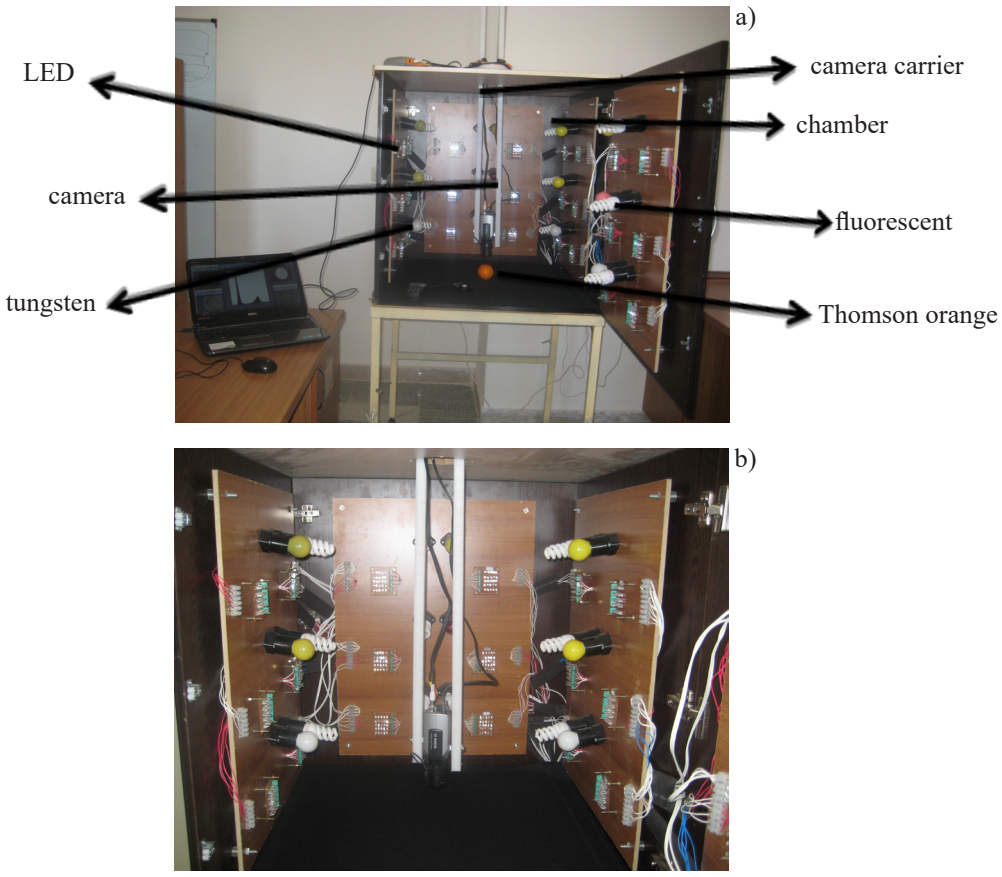

Figure 1. Image acquisition system chamber: (a) chamber overview, (b) in detail zoomed image.

lamps were uniformly distributed around the samples in order to remove any possible shadow. A dimmer was built for providing high and low illumination conditions. The digital camera was placed in the center of the image acquisition system, and was fixed during all the time at a distance of 15 cm between sample and digital camera. For optimal image acquisition, only lamps of white LED with a light intensity of 70.44 lux were selected.

Image segmentation

A simple yet effective algorithm for orange segmentation from background, was implemented as depicted in Fig. 2 flowchart. In Fig. 3, the peaks of the histogram from left to right are related to the high number of fruit and background color pixels, respectively. From Fig. 3, it can be seen that segmentation of fruit from the background could be easily accomplished with a proper thresholding method in the red component of color image. After choosing the proper segmentation threshold, a number of discriminant parameters (features) will be computed and their corresponding data will be saved in the input image database for future use while in the machine learning automatic regression phase. Despite selection of the best possible imaging conditions, segmented images still had the presence of artifacts (noise). Canny and Laplacian filters were employed for noise removal. Regarding Canny filter, edges are detected with local maximum gradient function $f(x,y)$. Gradient was computed using a derivative of a Gaussian filter. Two thresholds were used to identify strong and weak edges. Regarding Laplacian filter, edges were detected after filtering $f(x,y)$ using a Gaussian filter (Gonzalez *et al.*, 2004).

Image processing and feature extraction

After image segmentation, image processing was accomplished as described in detail in Fig. 4 block diagram, where efficient algorithms were programmed in MatLab language that were able to compute the following 14 features: eccentricity, roughness, red component value, blue component value, green component value, contrast, texture, area, perimeter, length/area, width, width/area, width/length, and length, from segmented fruit images (Fig. 4).

Artificial intelligence and machine learning procedures

Several artificial intelligence methods and algorithms were taken into account here: ANN, genetic algorithm (GA) and PSO, which are briefly described next.

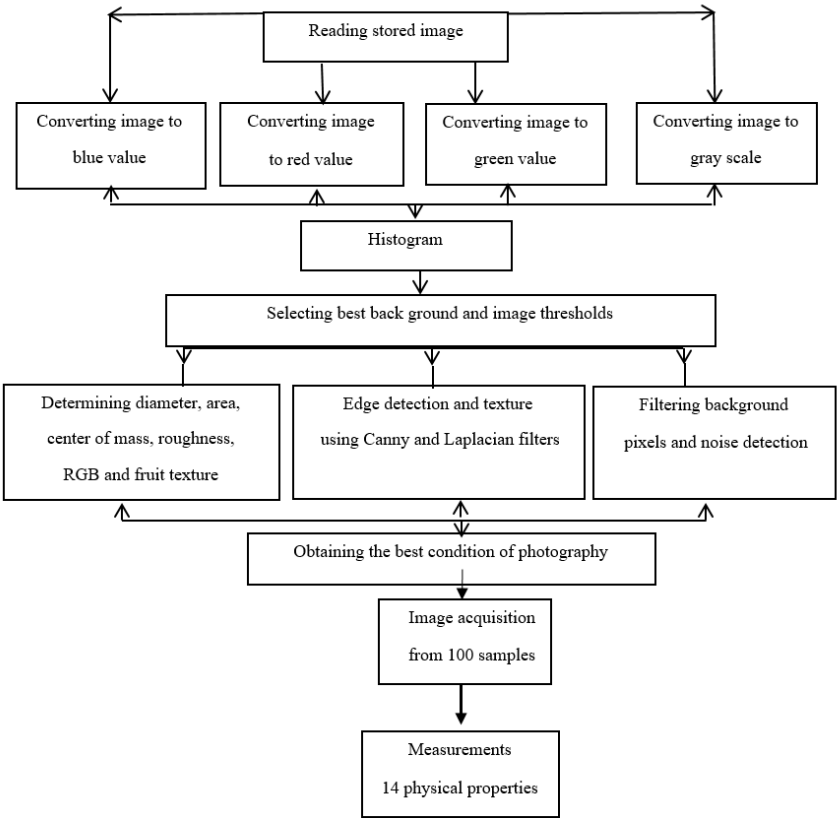

Figure 2. Image analysis system flowchart.

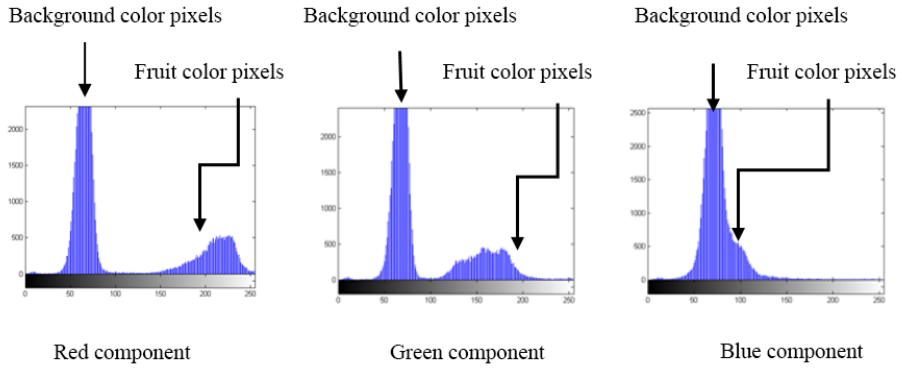

Figure 3. Histogram for each of the RGB components used in image segmentation and background removal.

Adjusting the neural network weights and bias terms ensures network accuracy. For this reason, a combination of PSO and GA algorithms was used. Next, it is explained in what way these three above mentioned methods are combined:

(a) Accuracy of neural network is related to weights (and bias) correct adjustment values.

(b) For the adjustment of weights in the neural network, a combination of PSO and GA algorithms was used.

(c) In each iteration two different steps must be done: 1) PSO algorithm adjusts neural network weights, based on mean square error (MSE); 2) GA algorithm adjusts neural network weights, also based on MSE too.

(d) Finally both PSO and GA algorithms MSE were compared over weights and optimal weights were selected at each iteration.

Artificial Neural Networks (ANN)

Nowadays, ANN are used in a wide range of problems in different domains such as, physics, medicine, engineering and finance. Three main reasons for this widely usage are: power of models, ease of use and high computational speed (Wen Sun, 2006). The basic

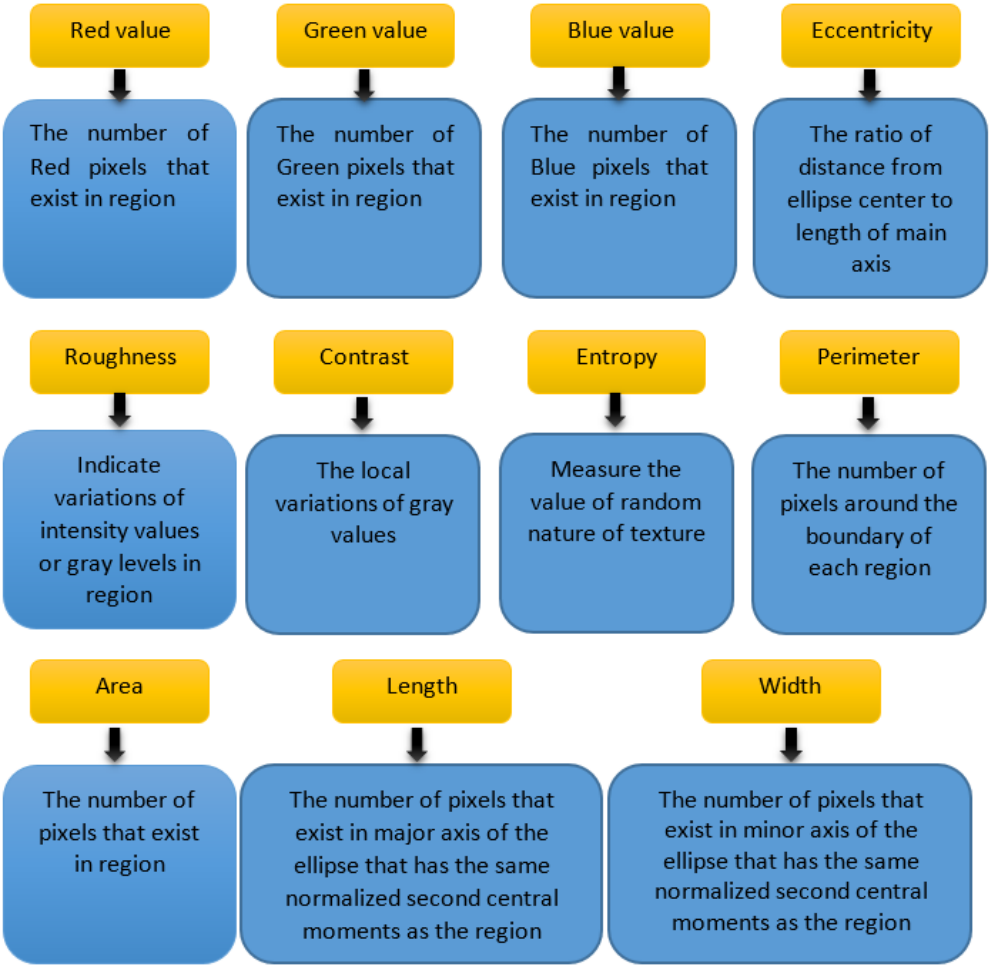

Figure 4. Feature extraction procedures summary.

structure of the well-known Elman Neural Networks includes three layers: input, recurrent *tansig* and output *purelin*. In this network, there was a feedback from output of first layer to its input. Two layers with *tansig* transfer function were used in this study. In addition, the hybrid PSO and GA was used for network training.

Genetic Algorithm (GA)

GA is a stochastic optimization method that mimics biological genetic evolutionary mechanisms. There are three main parameters in GA: probability of mutation, crossover and population size. The major advantages of GA, as compared to other conventional optimization approaches, are: (i) GA does optimization in a stochastic framework; (ii) GA does not limit the search space (Yuan *et al.*, 2014), making an exhaustive search.

Particle Swarm Optimization (PSO)

PSO is a robust stochastic optimization technique based on the evolution in time and intelligence of natural swarms in nature. It applies the concept of social interaction to problem solving. It was jointly developed in 1995 by James Kennedy (social-psychologist) and Russell Eberhart (electrical engineer). PSO takes into account a high number of agents (particles) that constitute a swarm moving around in the search space looking for an optimal solution and each particle is treated as a point in an n-dimensional space which adjusts its "flying" according to its own flying experience as well as the flying experience of other particles in swarm. Each particle keeps track of its own coordinates in the solution space which are associated with the best solution (fitness) that has been achieved so far by that particle. This value is called personal best, *pbest*. Another best value that is tracked by the PSO is the best value obtained so far by any particle in the neighborhood of that particle. This value is called *gbest*. The basic concept of PSO lies in accelerating each particle towards its *pbest* and the *gbest* locations, with a random weighted acceleration at each time step. Thus, the idea behind this scheme is that each particle tries to modify its position using the current positions, the current velocities, the distance between the current

position and *pbest*, the distance between the current position and *gbest* (Modenes *et al.*, 2012).

Taguchi experimental setup

PSO and GA, like other optimization algorithms, are mainly influenced by values of parameters. These parameters can be set by using different approaches such as full factorial experiment or manually. With an increase in the number of parameters, the number of experiments increases fast; for example with 6 parameters and 3 levels for each parameter one needs to perform 3^6=729 experiments. On the contrary, in Taguchi's proposed approach, a large number of decision variables would be tuned through a small number of experiments. This method divides parameters into noise and controllable parameters to minimize the effect of noise and determine optimal level of important controllable factors based on the concept of robustness. Taguchi's method applies two major tools which are the signal-to-noise ratio (SNR) and the orthogonal array. The goal is to maximize the SNR (Karimi *et al.*, 2011). The corresponding SNR (Phadke, 1989; Shokrollahpour *et al.*, 2011) is defined as:

$$S/N\ ratio = -10\log_{10}(objective\ function)^2 \quad (1)$$

Data generation and settings

An experiment was conducted to test the performance of the hybrid PSO, GA and ANN approach. Six factors and three levels for each one were selected following Taguchi approach, as presented in Table 1.

Hybrid of PSO-GA-ANN parameters tuning

The Taguchi method was used for statistical calibration of the parameters in algorithm. These experiments were implemented in MatLab (ver R2014a). The orthogonal array used with six factors and three levels in Taguchi method is L_{27}. L_{27} orthogonal array, results of experiment and MSE are presented in Table 2. The relative percentage deviation (RPD) is used as a common performance measure to setting parameters:

$$RPD = \frac{Algorithm_{sol} - Min_{sol}}{Min_{sol}} \times 100 \quad (2)$$

where $Algorithm_{sol}$ is result for a given algorithm and Min_{sol} is minimum result for all algorithms (Shokrollahpour *et al.*, 2011). The optimal levels of factors A, B, C, D, E, and F (see Table 1) become 3, 1, 2, 1, 1, and 3, respectively, being the number of neurons in first layer (A)=7, number of neurons in second layer (B)=2, maximum iteration (C)=400, crossover probability (D)=0.7, Mutation probability (E)=0.1, and swarm (population) size (F)=200.

Table 1. Factors and their levels in the hybrid ANN-PSO-GA system: Taguchi approach.

Factor	Value
Number of neurons in first layer (A)	3, 5, 7
Number of neurons in second layer (B)	2, 4, 6
Maximum iteration (C)	200, 400, 600
Crossover percentage (D)	0.7, 0.8, 0.9
Mutation percentage (E)	0.1, 0.15, 0.2
Swarm (population) size (F)	50, 100, 200

Results

Feature selection

Among all possible combinations of input features initially considered, three of them (the ratios of length/area, width/area and width/length) were selected as inputs to the Elman Neural Network.

Estimation of peel thickness

Table 3 shows true and mean±std estimated 100 orange peel thickness data, over the test set. Standard deviation of estimated peel thickness values was also included, for the 100 uniform random test set samples simulations averaged: on average, each orange # was used 20 times inside the test set.

In Table 4 the result of estimated orange peel thickness is shown based on levels that were achieved by Taguchi method, including the regression and error coefficients for the proposed automatic orange peel thickness estimation model. Mean and standard deviation of regression and error coefficient for the 100 uniform random test set samples simulations averaged are shown in Table 4; again, on average, each input orange sample is used 20 times in the test set. These performance indexes were computed from the following equation definitions (Liu *et al.*, 2013; Sabzi *et al.* 2013):

$$R^2 = 1 - \left\{\frac{\sum_{k=1}^{n}(X_k - X_0)^2}{\sum_{k=1}^{n}(X_k - X_m)^2}\right\} \quad (3)$$

$$X_m = \frac{1}{n}\sum_{k=1}^{n} X_k \quad (4)$$

$$MSE = \frac{1}{n}\sum_{k=1}^{n}(X_k - X_0)^2 \quad (5)$$

$$SSE = \sum_{k=1}^{n} (X_k - X_0)^2 \quad (6)$$

$$MAE = \frac{1}{n} \sum_{k=1}^{n} |X_k - X_0| \quad (7)$$

$$RMSE = \sqrt{\frac{1}{n} \sum_{k=1}^{n} (X_k - X_0)^2} \quad (8)$$

where X_k are the actual values, X_0 are the estimated values, X_m is the mean of the actual values and *n* is the number of estimates. The results achieved indicate that our hybrid automatic and non-intrusive model yielded significant reliable performance and generalization capability in the prediction task carried out.

Fig. 5 shows peel thickness prediction result of test data given by the hybrid PSO-GA-ANN system. From Fig. 5 it is clear that the proposed model achieves good generalization performance given that the PSO-GA is a good compromise for guaranteeing improvement in both stability and accuracy, and is a suitable and effective method for predicting the peel thickness of orange.

Regression analysis was conducted over the estimated peel thickness with respect to the measured (true) peel thickness obtained from the entire experiment sets. Fig. 6 depicts regression analysis, plotting true versus estimated orange peel thickness (mm) over the 100 orange database, test set. The highest R linear regression coefficient between the measured and estimated peel thickness was 0.92659.

Fig. 7 shows dispersion boxplots for (*true* - *estimated*) orange peel thickness (mm), over the 100 different orange image database. Boxplots for true-estimated peel thickness

Table 2. Taguchi method: the orthogonal array L_{27}, mean square error (MSE) (see Eq. 5) and relative percentage deviation (RPD) (see Eq. 2).

Experiments	Factors						MSE	RPD
	A	B	C	D	E	F		
1	1	1	1	1	1	1	0.037267	146.8503676
2	2	2	1	1	1	1	0.040510	168.3314566
3	3	3	1	1	1	1	0.037167	146.1879844
4	1	1	2	2	2	1	0.050727	236.0071537
5	2	2	2	2	2	1	0.015097	0.0000000
6	3	3	2	2	2	1	0.030404	101.3910048
7	1	1	3	3	3	1	0.043062	185.2354772
8	2	2	3	3	3	1	0.043622	188.9448235
9	3	3	3	3	3	1	0.052355	246.7907531
10	2	1	3	2	1	2	0.041832	177.0881632
11	3	2	3	2	1	2	0.032117	112.7376300
12	1	3	3	2	1	2	0.047423	214.1220110
13	2	1	1	3	2	2	0.048598	221.9050142
14	3	2	1	3	2	2	0.038179	152.8913029
15	1	3	1	3	2	2	0.056181	272.1335365
16	2	1	2	1	3	2	0.057866	283.2946943
17	3	2	2	1	3	2	0.053948	257.3425184
18	1	3	2	1	3	2	0.060486	300.6491356
19	3	1	2	3	1	3	0.034186	126.4423395
20	1	2	2	3	1	3	0.046347	206.9947672
21	2	3	2	3	1	3	0.024718	63.72789296
22	3	1	3	1	2	3	0.042946	184.4671127
23	1	2	3	1	2	3	0.048785	223.1436709
24	2	3	3	1	2	3	0.050995	237.7823409
25	3	1	1	2	3	3	0.026258	73.92859509
26	1	2	1	2	3	3	0.059170	291.9321720
27	2	3	1	2	3	3	0.033233	120.1298271

Table 3. True and estimated (mean±std) orange peel thickness values (mm), test set. Standard deviation (std) of estimated peel thickness values are included, for the 100 uniform random test set samples simulations averaged. On average, each orange number (#) is used 20 times inside the test set.

Orange #	True (mm)	Estimated (mm)	Orange #	True (mm)	Estimated (mm)	Orange #	True (mm)	Estimated (mm)
1	2.96	3.33±0.41	*35*	3.51	3.04±0.33	*69*	2.48	2.23±0.42
2	5.70	5.19±0.27	*36*	4.67	4.37±0.35	*70*	2.39	2.15±0.42
3	5.94	5.62±0.42	*37*	5.10	4.90±0.22	*71*	1.84	2.18±0.33
4	2.19	2.08±0.38	*38*	3.95	4.16±0.32	*72*	5.15	4.38±0.35
5	3.20	3.60±0.43	*39*	5.62	5.31±0.28	*73*	1.09	1.60±0.37
6	1.10	1.53±0.14	*40*	5.98	5.92±0.24	*74*	1.05	1.70±0.17
7	4.09	3.68±0.28	*41*	3.94	5.19±0.34	*75*	2.42	2.85±0.37
8	4.58	3.83±0.33	*42*	6.04	5.78±0.31	*76*	2.44	2.92±0.38
9	4.80	4.21±0.30	*43*	6.88	5.87±0.22	*77*	2.14	2.16±0.31
10	2.60	2.63±0.44	*44*	5.01	4.52±0.32	*78*	3.03	3.91±0.34
11	3.32	3.22±0.32	*45*	2.59	3.88±0.33	*79*	4.91	4.39±0.48
12	4.14	5.07±0.27	*46*	4.55	5.48±0.27	*80*	3.56	3.58±0.36
13	6.05	4.74±0.29	*47*	5.73	5.99±0.35	*81*	4.76	4.53±0.30
14	5.84	5.59±0.17	*48*	3.55	4.44±0.27	*82*	2.45	2.25±0.41
15	2.79	3.03±0.43	*49*	5.03	5.50±0.24	*83*	3.48	3.75±0.34
16	4.30	4.47±0.21	*50*	3.25	4.02±0.34	*84*	4.62	5.30±0.30
17	7.19	5.45±0.18	*51*	5.33	5.11±0.31	*85*	4.36	4.04±0.25
18	6.46	5.94±0.24	*52*	4.39	4.67±0.33	*86*	1.03	1.58±0.31
19	6.64	6.07±0.20	*53*	6.35	5.88±0.27	*87*	3.11	3.17±0.41
20	6.89	6.04±0.20	*54*	3.09	3.43±0.33	*88*	3.77	3.23±0.36
21	3.75	3.33±0.32	*55*	7.00	5.81±0.19	*89*	3.20	3.69±0.35
22	4.90	4.60±0.41	*56*	4.88	5.53±0.26	*90*	2.35	3.20±0.33
23	7.15	6.11±0.14	*57*	5.14	5.33±0.29	*91*	1.94	2.68±0.36
24	7.37	6.46±0.14	*58*	6.74	6.10±0.16	*92*	3.67	3.97±0.32
25	5.29	5.49±0.29	*59*	5.00	5.51±0.32	*93*	2.19	2.70±0.38
26	3.38	3.62±0.30	*60*	4.32	4.79±0.26	*94*	4.26	4.15±0.28
27	3.73	4.03±0.30	*61*	3.75	4.04±0.34	*95*	5.23	4.41±0.28
28	3.83	2.82±0.38	*62*	4.40	3.17±0.47	*96*	4.52	4.82±0.32
29	4.23	4.97±0.29	*63*	3.67	4.36±0.26	*97*	3.44	4.11±0.37
30	5.30	4.74±0.35	*64*	1.34	1.83±0.17	*98*	4.25	5.07±0.32
31	3.23	4.00 ±0.29	*65*	2.36	2.23±0.34	*99*	5.70	5.56±0.24
32	5.14	4.81±0.24	*66*	2.22	3.06±0.37	*100*	6.87	5.59±0.29
33	5.42	5.09±0.34	*67*	2.04	2.09±0.38			
34	4.43	4.39±0.31	*68*	2.40	2.63±0.41			

values were computed over the test set. To our best knowledge, taking into account the non-intrusive nature of the peel thickness estimation process, results shown in Fig. 7 are remarkable, since 92 out of 100 orange samples had error values under 1 mm in peel thickness estimation.

To conclude the estimation of peel thickness results section, Fig. 8 shows boxplots for the various error measures and coefficients, including SSE, MSE, MAE, RMSE, R, and R^2, computed over the uniform random orange test set, in which, again, experiments were uniform random repeated 100 times, resulting in 2000 test oranges, since each different orange # was used 20 times on average over the test set.

Potential application to an industrial case study

Determination of ranked factors

Appropriate design of the parameters and operators has a significant impact on the efficiency of the hybrid

Table 4. Regression and error coefficients for the proposed automatic orange peel thickness estimation model. Mean ± standard deviation (std) and best case values of regression and error coefficients for the 100 uniform random test set samples simulations averaged. On average, each orange sample was used 20 times (test set). The sum square error (SSE), the mean absolute error (MAE), the coefficient of determination (R^2), the RMSE, and the mean squared error (MSE) were employed as performance indicators to evaluate prediction capability of the model.

	R^2	SSE	MAE	MSE	RMSE
Mean ± std	0.854±0.052	0.766±0.209	0.159±0.023	0.038±0.010	0.193±0.027
Best case[1]	0.963	0.678	0.132	0.022	0.148

[1]Optimal results included for comparison purposes.

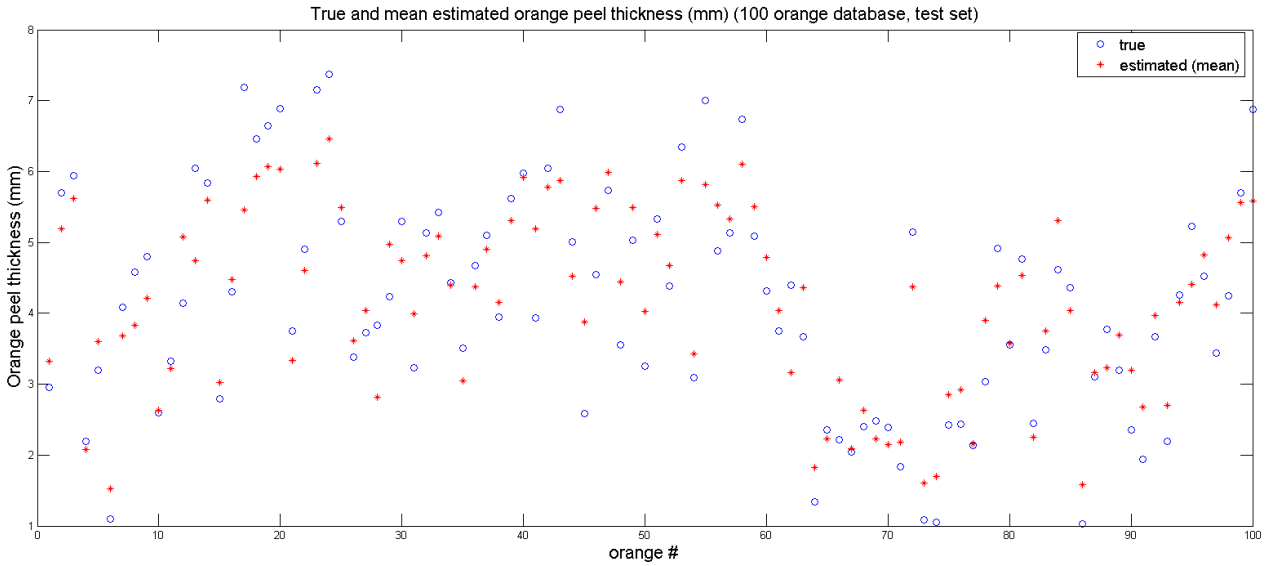

Figure 5. True and mean estimated orange peel thickness (mm) over the 100 orange database. Test set: experiments were uniformly random repeated 100 times, resulting in 2000 test oranges (each different orange # was used 20 times on average over the test set).

of PSO-GA-ANN. In this work, the behavior of the different parameters of the proposed hybrid PSO-GA-ANN system was studied. Among the several methods to statistically calibrate algorithms parameters, the Taguchi method was used for this purpose. Table 5 illustrates the computed SNR data and shows the order of effective factors in rank row. It can be inferred from previous table that F factor was the most effective factor. In decreasing effective order, factors were ranked as follows: F, A, C, B, D and E.

Grading system prototype proposal

The non-intrusive orange peel thickness grading system prototype is depicted in Fig. 9. Oranges with different peel thicknesses were placed on conveyor belt and the camera took images over them. Images captured were then transferred to the computer for analysis by proper algorithms. After analysis, fruits were divided into two groups: fruit with high peel thickness and fruit with low peel thickness. Two independent lines were built to transfer oranges with different peel thickness towards the corresponding packaging areas. Oranges with high peel thickness can be used for preparation of jams and oil extraction, while oranges with low peel thickness can be used for fresh juice consumption.

Fig. S1 [suppl] includes the visualization of the 100 Thomson orange image database used in this research for automatic peel thickness estimation.

Discussion

Automatic estimation of peel thickness from computer vision is a new research field and as such not may examples in the literature do exist. In this work, an accurate hybrid automatic non-intrusive method based on PSO, GA and ANN was proposed for prediction of peel thickness in Thomson

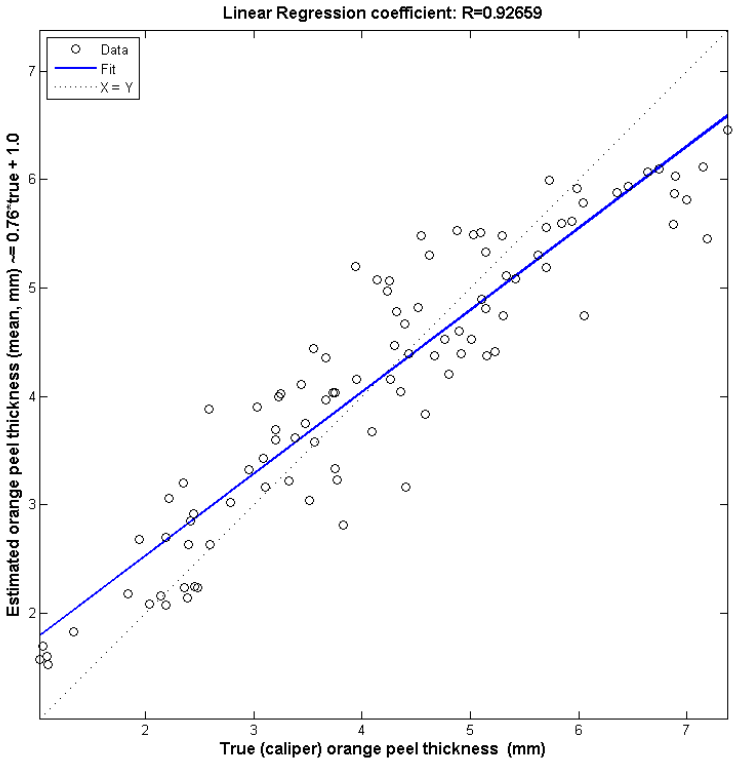

Figure 6. Linear regression plot example of true *vs* estimated orange peel thickness (mm) over the 100 orange database. Test set: experiments were uniformly random repeated 100 times, resulting in 2000 test oranges (each different orange # was used 20 times on average over the test set).

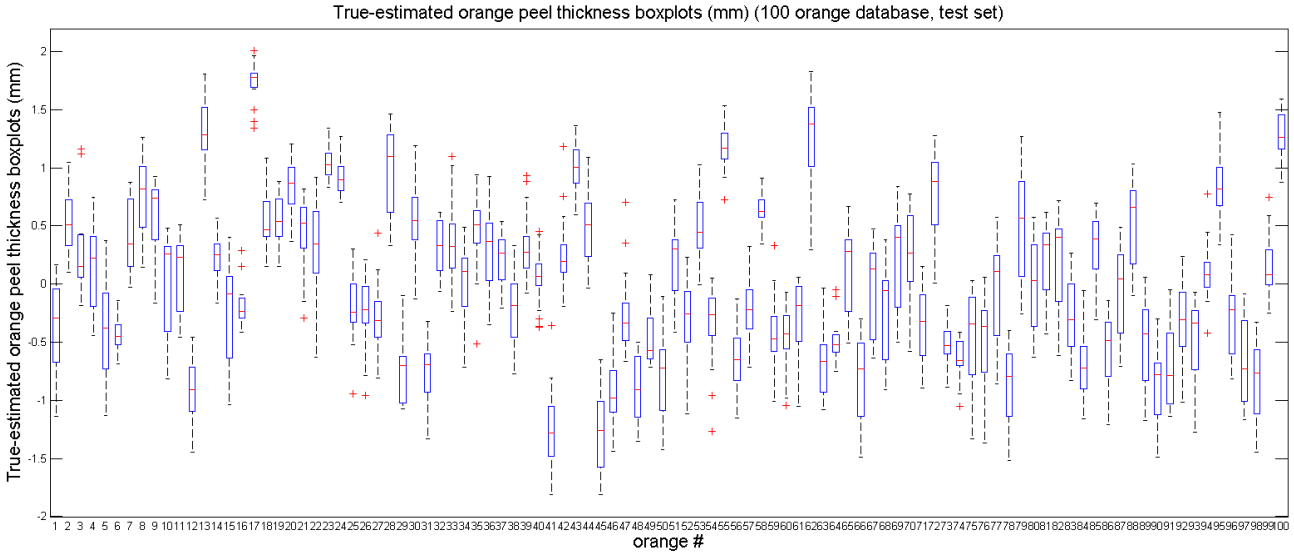

Figure 7. Peel thickness boxplots for the 100 orange database. True-estimated peel thickness values (test set): 100 uniform random test set samples simulations averaged. On average, each input orange # was used 20 times.

orange, conveniently validated with statistical valid remarkable results computed over the test set, including boxplots of both true–estimated orange peel thickness and of main performance indexes.

Selected features

As mentioned in the Results section, the three most discriminative selected features were: the ratios

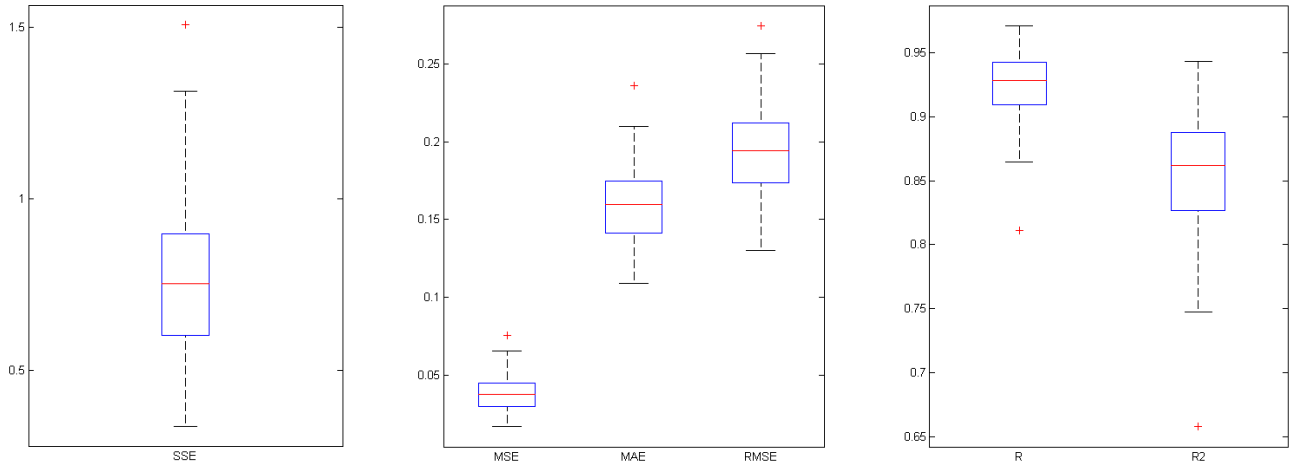

Figure 8. Error coefficients boxplots, for SSE, MSE, MAE, RMSE, R and R^2: experiments were uniformly random repeated 100 times, resulting in 2000 test oranges. Each different orange # was used 20 times on average, over the test set.

of length/area, width/area and width/length. It can be concluded that thickness estimation needs to use ratios of geometric properties. In addition, skin thickness of this orange variety could not be estimated based on color features. We believe this is due to the fact that skin orange color is an inherent property, so all fruits belonging to same variety have very similar skin color features.

Parameter optimization

As mentioned in the Results section, there are 729 different states for value adjustment over the following six parameters A, B, C, D, E and F (see Table 1); Taguchi method selected 27 optimal states. Results showed that A and B were 7 and 2, respectively. This fact means that the model is quite simple since there are only 7×2=14 possible network connections (weights) between layers 1 and 2. C was set to 400, meaning that the optimal number of iterations is less than 400 because higher iteration numbers only cause a waste of time or even overfitting in the worst case. D based on Taguchi method was set to 0.7, being a reasonable value since if this parameter had a higher amount chromosome might not have a good matching. The value of E was set to 0.1 so as to avoid algorithm is caught in local minima and this way achieve convergence to a new better final solution. F was set to 200, assuring better solutions under high population schemes (Mitchell, 1999).

Table 5. Signal to noise ratios and the order of effective factors used, following Taguchi methodology. Factors A to F are defined in Table 1.

Level	A	B	C	D	E	F
1	-44.68	-43.14	-46.42	-44.30	-44.65	-47.07
2	-46.53	-45.84	-43.56	-44.85	-45.70	-44.52
3	-43.61	-45.98	-44.72	-45.68	-44.59	-43.22
Delta	2.91	2.84	2.86	1.38	1.11	3.85
Rank	2	4	3	5	6	1

Peel thickness estimation: accuracy

Table 3 and Fig. 5 show that for almost all 100 input orange image samples, peel thickness estimation values have errors under 1.0-1.5 mm (Fig. 7), which we believe is a remarkable estimation accuracy for a non-intrusive computer vision approach. Besides, Fig. 8 shows error indexes, R and R^2 parameters boxplots. These boxplots are quite compact, meaning that this method achieves similar results over different simulation iterations, thus it can be concluded that the system is stable and reliable. Two things are worth noting in order to keep high accuracy estimation indexes: (i) true orange peel thickness measurements should be done with high accuracy, for obvious reasons, given the high accuracy of estimated peel thickness values; and (ii) high precision should be applied in the selection of critical factors and their levels in optimization algorithms.

Comparison with previous studies from the literature

Despite each input fruit image database is different, Table 4 shows regression results and error coefficients for the proposed automatic orange peel thickness estimation system, for the best run among all runs (over test set) for comparison purposes. As one can see, this method has promising results in peel thickness estimation.

Jafari *et al.* (2014) recognized orange skin thickness based on visual texture coarseness. In fact they believe

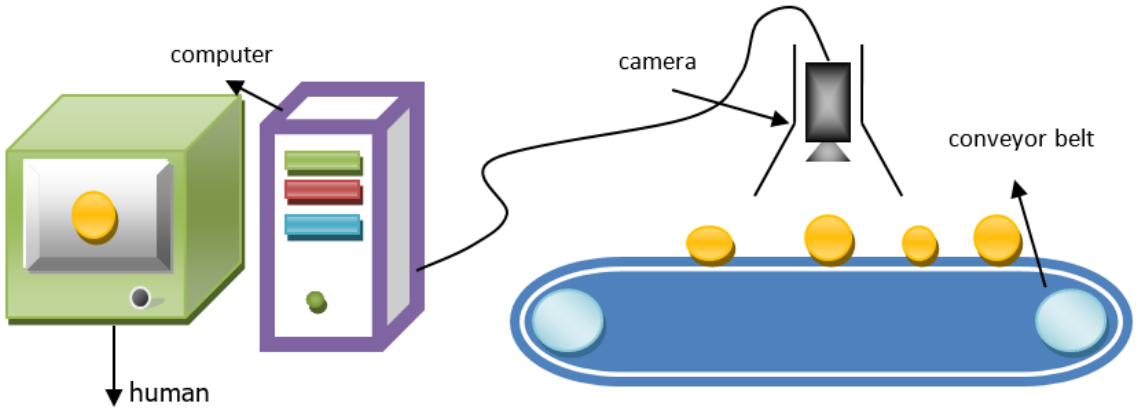

Figure 9. Layout of an automatic non-intrusive orange peel-thickness computer fruit sorting system prototype.

that an orange with coarser surfaces has thicker peel than other oranges. They did imaging in two states of illumination: directional and omnidirectional. Results show that the coefficient of determination between coarseness factor and thickness for two illumination states, either directional or omnidirectional, were 0.903 and 0.683, respectively. There were several adjustable parameter and variable definitions that affected the results in this study. These variables were: 1) illumination, 2) selected color component, 3) size of the moving kernels and 4) discrimination length of the strips. Bad adjustment and incorrect selection of above variables have direct effect on accuracy of the prediction. Use of this method for grading in the production line has a potential limitation: it is based on high resolution images while in the production line images are often captured with medium-low resolution, in order to increase speed.

Río-Segade *et al.* (2011) used berry peel thickness to estimate anthocyanin extractability in wine grapes. Peel thickness was determined by mechanical equipment and anthocyanin extracted using several chemicals. Results show that linear regression coefficients between berry skin thickness and anthocyanin extractability for Mencía grape variety from several vineyards were highly variable between 0.259 and 0.683, what can pose an applicability problem. On the other hand, given the need of both mechanical equipment and various chemicals, computer vision grading based on peel thickness to detect anthocyanin cannot be used in and automatic non-intrusive environment.

In another interesting research, Williams *et al.* (2007) analyzed the relationship between bark thickness and diameter at breast height in four tree varieties. The minimum and maximum values of the coefficient of determination found were 0.005 and 0.802, respectively. In this study, again like previous one, experiments have been performed manually, thus experiments made by different persons can have different output results depending on each person experience and skills. At the same time, thickness may be different in various parts of tree, so this fact may have an effect over results.

Homutová & Blažek (2006) studied apple skin thickness computed based on both direct measurement and mean scores of panelists, 10 people. For this purpose, six different apple types were selected. Results show that the regression coefficient between true and estimated skin thickness was 0.91. For systematic grading based on peel thickness the use of panelists is not applicable in packaging factories since fatigue, visual error, and physical condition of the person might have an effect on estimation accuracy. Besides, speed is a critical parameter in packaging factories, thus resulting not practical for grading purposes in the food industry.

Morgan *et al.* (2005) studied the relationship between peel thickness of "Hamlin" oranges and some mineral contain in it. Results show that the regression coefficient for different parameter pairs (leaf potassium concentration and fruit peel thickness, fruit peel potassium concentration and mean fruit peel thickness, mean fruit peel thickness and mean fruit diameter) were 0.704, 0.898, 0.732, respectively. The relationship between peel thickness and mineral contain can play an important role in the packaging industry, since based on peel thickness one can select oranges that have, for instance, high potassium without the use of any destructive methods, by using an imaging system, and image processing. In this study, all experiments were done manually, without the use of any imaging system, image processing or image analysis, thus it cannot be used for grading purposes in the packaging industry.

As it can be seen from Table 4, in the optimal case over the test set, the coefficient of determination between orange peel thickness and the ratios of length/area, width/area and width/length features was above

0.96, all automatic and non-intrusive. As a result, it can be inferred that the here proposed method performed better than previous ones found in the literature, but please take into account that image databases, fruits (not always orange), orange varieties and applications could differ a lot among the papers here analyzed.

To conclude, we believe that the automatic and non-intrusive Thomson orange peel thickness system proposed in this study could be potentially extended under real conditions in the sorting food industry, to judge from the accuracy of results achieved, but in order to maintain similar low peel thickness estimation error levels, the following should be carefully taken into account: (i) use of a camera with medium resolution if real time limitation permits to do so; (ii) locate the camera in a suitable distance from fruit, in such a way that real size of fruit is captured; (iii) appropriate homogeneous and fixed lighting condition, with limited light disturbances; and (iv) use of a suitable color as the background, omitting any possible light reflectance.

References

Adelkhani A, Beheshti B, Minaei S, Javadikia P, Ghasemi-Varnamkhasti M, 2013. Taste characterization of orange using image processing combined with ANFIS. Measurement 46: 3573-3580. https://doi.org/10.1016/j.measurement.2013.06.052

Blasco J, Aleixos N, Molto E, 2003. Machine vision system for automatic quality grading of fruit. Biosyst Eng 85 (4): 415. https://doi.org/10.1016/S1537-5110(03)00088-6

Fan FH, Ma Q, Ge J, Peng QY, Riley WW, Tang SZ, 2013. Prediction of texture characteristics from extrusion food surface images using a computer vision system and artificial neural networks. J Food Eng 118: 426-433. https://doi.org/10.1016/j.jfoodeng.2013.04.015

Fu L, Sun S, Li R, Wang S, 2016. Classification of kiwifruit grades based on fruit shape using a single camera. Sensors 16: 1-14. https://doi.org/10.3390/s16071012

Gonzalez RC, Woods RE, Eddins SL, 2004. Digital image processing using MATLAB. Prentice Hall.

Homutova I, Blazek J, 2006. Differences in fruit skin thickness between selected apple (Malus domestica Borkh.) cultivars assessed by histological and sensory methods. Hort Sci (Prague) 33 (3): 108-113. https://doi.org/10.17221/3747-HORTSCI

Jafari A. Fazayeli A, Zarezadeh MR, 2014. Estimation of orange skin thickness based on visual texture coarseness. Biosys Eng 117: 73-82. https://doi.org/10.1016/j.biosystemseng.2013.08.010

Karimi N, Zandieh M, Najafi AA, 2011. Group scheduling in flexible flow shops: a hybridised approach of imperialist competitive algorithm and electromagnetic-like mechanism. Int J Prod Res 49 (16): 4965-4977. https://doi.org/10.1080/00207543.2010.481644

Karimi H, Navid H, Mahmoudi A, 2015. Online laboratory evaluation of seeding-machine application by an acoustic technique. Span J Agric Res 13 (1): e0202. https://doi.org/10.5424/sjar/2015131-6050

Leiva-Valenzuela GA, Lu R, Aguilera JM, 2013. Prediction of firmness and soluble solids content of blueberries using hyperspectral reflectance imaging. J Food Eng 115: 91-98. https://doi.org/10.1016/j.jfoodeng.2012.10.001

Liu S, Xu L, Li D, Li Q, Jiang Y, Tai H, Zeng L, 2013. Prediction of dissolved oxygen content in river crab culture based on least squares support vector regression optimized by improved particle swarm optimization. Comput Electron Agr 95: 82-91. https://doi.org/10.1016/j.compag.2013.03.009

Marchal PC, Gila DM, García JG, Ortega JG, 2013. Expert system based on computer vision to estimate the content of impurities in olive oil samples. J Food Eng 119: 220-228. https://doi.org/10.1016/j.jfoodeng.2013.05.032

Mellit A, Kalogirou SA, 2014. MPPT-based artificial intelligence techniques for photovoltaic systems and its implementation into field programmable gate array chips: Review of current status and future perspectives. Energy 70: 1-21. https://doi.org/10.1016/j.energy.2014.03.102

Mitchell M, 1999. An introduction to genetic algorithms. The MIT Press, Cambridge, MA, USA. https://mitpress.mit.edu/books/introduction-genetic-algorithms

Modenes AN, Espinoza-Quiñones FR, Trigueros DEG, Pietrobelli JM, Lavarda FL, Ravagnani MA, Bergamasco R, 2012. Binary adsorption of a Zn(II)-Cu(II) mixture onto *Egeria densa* and *Eichhornia crassipes*: Kinetic and equilibrium data modeling by PSO. Sep Sci Technol 47: 875-885. https://doi.org/10.1080/01496395.2011.627407

Mohapatra A, Shanmugasundaram S, Malmathanraj R, 2017. Grading of ripening stages of red banana using dielectric properties changes and image processing approach. Comput Electron Agr 143: 100-110. https://doi.org/10.1016/j.compag.2017.10.010

Morgan KT, Rouse RE, Roka FM, Futch SH, Zerri M, 2005. Leaf and fruit mineral content and peel thickness of 'Hamlin' orange. Proc Fla State Hort Soc 118: 19-21.

Mottaghitalab M, Nikkhah M, Darmani-Kuhi H, López S, France J, 2015. Predicting methionine and lysine contents in soybean meal and fish meal using a group method of data handling-type neural network. Span J Agric Res 13 (1): e0601. https://doi.org/10.5424/sjar/2015131-5877

Naganur HG, Sannakki SS, Rajpurohit VS, Arunkumar R, 2012. Fruits sorting and grading using fuzzy logic. Int J Adv Res Comput Eng Technol 1 (6): 117-122.

Phadke MS, 1989. Quality engineering using robust design. Prentice-Hall, Englewood Cliffs, NJ, USA.

Rio-Segade S, Giacosa S, Gerbi V, Rolle L, 2011. Berry skin thickness as main texture parameter to predict anthcyanin

extractability in winegrapes. Food Sci Technol 44: 192-398.

Rungpichayapichet P, Nagle M, Yuwanbun P, Khuwijitjaru P, Mahayothee B, Muller J, 2017. Prediction mapping of physicochemical properties in mango by hyperspectral imaging. Biosyst Eng 159: 109-120. https://doi.org/10.1016/j.biosystemseng.2017.04.006

Sabzi S, Javadikia P, Rabani H, Adelkhani A, 2013. Mass modeling of Bam orange with ANFIS and SPSS methods for using in machine vision. Measurement 46: 3333-3341. https://doi.org/10.1016/j.measurement.2013.06.005

Shin JS, Lee WS, Ehsani R, 2012. Postharvest citrus mass and size estimation using a logistic classification model and a watershed algorithm. Biosyst Eng 113: 42-53. https://doi.org/10.1016/j.biosystemseng.2012.06.005

Shokrollahpour E, Zandieh M, Dorri B, 2011. A novel imperialist competitive algorithm for bi-criteria scheduling of the assembly flowshop problem. Int J Prod Res 49: 3087-3103. https://doi.org/10.1080/00207540903536155

Thendral R, Suhasini A, 2017. Automated skin defect identification system for orange fruit grading based on genetic algorithm. Current Sci 112 (8): 1704-1711. https://doi.org/10.18520/cs/v112/i08/1704-1711

Tong JH, Li JB, Jiang HY, 2013. Machine vision techniques for the evaluation of seedling quality based on leaf area. Biosyst Eng 115: 369-379. https://doi.org/10.1016/j.biosystemseng.2013.02.006

Wen Sun D, 2006. Thermal food processing. Taylor & Francis, NY.

Williams VL, Witkowski ETF, Balkwill K, 2007. Relationhip between bark thickness and diameter at breast height of six tree species used medicinally in South Africa. S Afr J Bot 73: 449-465. https://doi.org/10.1016/j.sajb.2007.04.001

Yuan J, He C, Gao W, Lin J, Pang Y, 2014. A novel hard decision decoding scheme based on genetic algorithm and neural network. Optik 125 (14): 3457-3461. https://doi.org/10.1016/j.ijleo.2014.01.035